Neoplasma 2024; 71(4): 359–373

doi:10.4149/neo_2024_231219N653

WTAP/CCND1 axis accelerates esophageal squamous cell carcinoma progression by MAPK signaling pathway

Hong ZHANG[1], Xiaojing ZHANG[2], Yan ZHANG[3], Jianhua WU[4], Jiali LI[1,*], Baoen SHAN[1,*]

[1]Research Center, The Fourth Affiliated Hospital of Hebei Medical University, Shijiazhuang, Hebei, China; [2]Traditional Chinese Medicine Nursing Clinic, Shijiazhuang People's Hospital, Shijiazhuang, Hebei, China; [3]Cytology Department, The Fourth Affiliated Hospital of Hebei Medical University, Shijiazhuang, Hebei, China; [4]Laboratory Animal Center, The Fourth Affiliated Hospital of Hebei Medical University, Shijiazhuang, Hebei, China

**Correspondence: jialifushan@163.com; baoenshan1962@sina.com*

Received December 19, 2023 / Accepted June 24, 2024

N6-methyladenosine (m6A) methylation, as a new regulatory mechanism, has been reported to be involved in diverse biological processes in recent years. Wilms tumor 1-associated protein (WTAP), as the key member of m6A methylation, has been proven to participate in tumorigenesis. Here, we studied the expression of WTAP and its potential mechanism involved in the development of esophageal squamous cell carcinoma (ESCC). We detected the expression of WTAP and its correlation with clinicopathological features, and we determined the function of WTAP on ESCC cells by MTS assay, colony formation, scratch wound healing assay, Transwell assay, and subcutaneous xenograft assay. We used mRNA sequencing technology to screen candidate downstream targets for WTAP and investigated the underlying mechanism of CCND1 in ESCC promotion through a series of rescue assays. An elevated expression of WTAP in ESCC malignancy indicated a worse prognosis. WTAP promoted the proliferation and metastasis of ESCC cells, and CCND1 was identified as the potential downstream effecter of WTAP. Moreover, WTAP modulated ESCC progression through a MAPK pathway-dependent pattern. Our research suggested that WTAP promoted both proliferation and metastasis of ESCC by accelerating the expression of CCND1 via the MAPK signaling pathway, indicating that WTAP may be a candidate prognostic biomarker for ESCC and also will be a promising strategy for ESCC cancer therapy.

Key words: N6-methyladenosine (m6A); Wilms tumor 1-associated protein (WTAP); esophageal squamous cell carcinoma (ESCC), cyclin D1 (CCND1), mitogen-activated protein kinase (MAPK)

Esophageal cancer (EC), one of the most common malignant tumors of the digestive tract in adults, ranks seventh among the leading causes of tumor-related death globally [1]. Due to the high rates of recurrence and metastasis, patients with EC have a low 5-year survival rate [1]. However, the tumor burden from EC is mainly concentrated in Asia, especially in China [2]. Owing to the different living habits from those of Western countries, the pathological type of EC with the highest incidence in China is squamous cell carcinoma (ESCC), which occurs mostly in the middle and lower esophagus and shows a certain familial aggregation and worse prognosis [3]. Although the treatment for ESCC has made great progress in recent decades, ranging from surgery, radiotherapy, and chemotherapy, the outcomes of ESCC are still undesirable [4]. Therefore, understanding the molecular mechanisms underlying ESCC development is critical to facilitate future diagnosis and treatment to develop more effective therapeutic strategies and prognostic biomarkers to reduce the mortality of this malignancy.

Generally speaking, epigenetic modification refers to reversible chemical modifications that occur on genomic DNA or histones to control cell differentiation and development by regulating gene expression [5]. Recently, growing studies have shifted their focus to chemical modifications on RNA, which was proven to play essential roles in human life not only by transmitting genetic information from DNA to protein but also by regulating a variety of biological processes. N6-methyladenosine (m6A) is the most prevalent internal modification in polyadenylated mRNAs and is considered a crucial determinant in posttranscriptional regulation of mRNA stability, mRNA splicing, and mRNA translation control [6–9]. Accumulating evidence has uncovered that m6A modifications in mRNAs or non-coding RNAs regulate RNA fate and are essential for most bioprocesses

including tissue progression, stem cells self-renewal and differentiation, circadian rhythm, tumorigenesis, maternal-to-zygotic transition, and so on [10]. m6A mRNA methylation is catalyzed by a multicomponent methyltransferase complex, consisting of a METTL3 and METTL14 heterodimeric enzymatic core and their regulatory factor, WTAP [11–14]. METTL3 is a key component of methyltransferase, acting as the S-adenosine methionine binding subunit, while METTL14 provides a critical RNA-binding scaffold to recognize substrates [15], and WTAP is essential to the stability of METTL3 and METTL14 and is further involved in their localization into nuclear speckles [13]. However, the research on m6A modification and the mechanism of m6A's involvement in the development of ESCC is still in its infancy.

Wilms tumor 1-associated protein (WTAP) is a universally expressed nuclear protein that was first identified to interact specifically with Wilms tumor 1, a protein that plays a key role in the normal evolvement of the genitourinary system [16]. Recent studies have shown that WTAP plays an essential role in regulating various physiological and pathological processes such as cell cycle, proliferation, apoptosis, RNA splicing, and m6A modification [12–13, 17–20]. In addition, growing evidences have confirmed that WTAP acted as an important oncogene, and is associated with various malignant tumors, including gastric cancer, acute myelogenous leukemia, colorectal cancer, glioblastoma, renal cell carcinoma, glioma, hepatocellular carcinoma, osteosarcoma, bladder cancer, pancreatic cancer, lymphoma, and cholangiocarcinoma [21–32]. Nevertheless, whether WTAP expression in ESCC is associated with the progression of malignancy still remains unknown.

CCND1, as the most famous member of the D-type cyclin proteins family, was considered as a critical element to regulate cell cycle progression [33]. Abnormal expression of CCND1 in the initial stage of a malignant tumor can lead to chromosome rearrangement and abnormal gene amplification, identifying that CCND1 may play an important role in the process of carcinogenesis [34–36]. In our study, we selected CCND1 as the key downstream target of WTAP and further confirmed the regulation function of CCND1 in the development of ESCC mediated by WTAP.

The MAPK pathway is the most dysregulated pathway involved in many cancers including ESCC [37]. Based on the KEGG analysis from our mRNA-seq, the MAPK pathway was regarded as the most important involved pathway in WTAP-dependent ESCC progression. The phosphorylation status of MAPK pathway-related molecules such as RAF, MEK, ERK was assessed to determine whether the MAPK pathway was activated and involved in WTAP-promoted ESCC progression.

Patients and methods

Public datasets. The Gene Expression Profiling Interactive Analysis (GEPIA) database (http://gepia.cancer-pku.cn/) was adopted to compare WTAP expression between multiple cancer types and matched normal tissues. The Cancer Genome Atlas (TCGA) dataset (https://cancergenome.nih.gov/) was used to compare the expression pattern of WTAP in ESCC tissues and the paired normal tissues.

Patients and specimens. The tissue samples were taken from 40 patients diagnosed with ESCC together with concurrent surgical resection from 2021 to 2022 at the Fourth Hospital of Hebei Medical University (Shijiazhuang, China). None of the patients received any treatment before surgery. Immediately after excision, the tissue samples were stored in liquid nitrogen for the following qRT-PCR or Western blotting detection and placed in 4% formalin for immunohistochemistry staining. This study was approved by the Research Ethics Committee of the Fourth Hospital of Hebei Medical University (approval no. 2021KY147), and all the patients signed the informed consent before surgery.

Cell lines and cell culture. Human ESCC cell lines (KYSE150, KYSE30, TE1, KYSE410, Eca109, and KYSE170) were purchased from Procell Life Science & Technology Co., Ltd. (Wuhan, Hubei, China). KYSE150 cell line was cultured with 45% RPMI-1640 medium (Gibco, USA) and 45% F12 (Procell, China) supplemented with 10% FBS (FBS; Biological Industries, Beit-Haemek, Israel) and 1% penicillin-streptomycin (Solarbio, China). KYSE30 cell line was cultured with 45% RPMI-1640 medium and 45% F12 supplemented with 10% FBS, 1% glutamax (Invitrogen, USA) and 1% penicillin-streptomycin. TE1, KYSE410, and Eca109 were cultured in RPMI-1640 medium containing 10% FBS and 1% penicillin-streptomycin. KYSE170 cell line was cultured in DMEM medium (Gibco, USA) containing 10% FBS and 1% penicillin-streptomycin. All the ESCC cell lines were incubated at 37 °C in humidified air containing 5% carbon dioxide. Morphological characteristics and proliferation ability have been detected on the six cell lines once a month, to ensure the repeatability and authenticity of this experiment.

Clinical tissue chip array samples. An ESCC tissue chip array, including 108 ESCC tissues and 72 matched adjacent tissues (HEsoS180Su11-M-081) was acquired from Outdo Biotech Corporation (Shanghai, China). The clinicopathological features and survival data of the patients were gained through follow-up data. All patients enrolled in this study signed a written informed consent and accepted the approved protocol by the Institutional Review Board of Shanghai Outdo Biotech Corporation (license number: SHYJS-CP-2004003).

RNA transfection. The human small interfering RNA (siRNA) oligonucleotides specifically directed against WTAP (siWTAP-1, siWTAP-2, and siWTAP-3) and siRNA negative control (siNC) were designed and provided by RiboBio (Guangzhou, China). The sequence of siRNA is as follows: siWTAP-1: 5'-GGAACAGACTAAAGACAAA-3'; siWTAP-2: 5'-CTAAGAGAGTCTGAAGAAA-3'; siWTAP-3: 5'-GAAGCATATGTACAAGCTT-3'. Cultured

KYSE150 and KYSE30 cells were transfected with 100 pmol siRNA in a 6-well plate by Ribo FECT TMCP Transfection (RiboBio, China) according to the manufacturer's protocol.

Plasmid transfection. For overexpression of WTAP or CCND1 in ESCC cells, the expression plasmid for WTAP (HX-H-OELV-13613-ZL, termed as oe-WTAP) or CCND1 (HX-H-OELV-00839-ZL, termed as oe-CCND1) and empty vector (termed as oe-Vector) were conducted by Haixing Biosciences (Suzhou, China). Cultured TE1 and KYSE410 cells were transfected with plasmid by jet PRIME Transfection Reagent (Polyplus, France).

RNA extraction and quantitative real-time reverse transcription PCR (qRT-PCR). Following the manufacturer's instructions, total RNA was extracted from tumor tissues, corresponding normal tissues, and cell lines using TRIzol Reagent (Invitrogen, USA). cDNA was synthesized by using GoScript™ Reverse Transcription Mix (Promega, USA), followed by an amplification reaction with GoTaq® qPCR Master Mix (Promega, USA) according to the manufacturer's protocol. The relative mRNA expression was calculated by the comparative CT method [38], with the normalization to GAPDH. All primers are summarized in Supplementary Table S1. All the samples were run in triplicate.

Western blotting analysis. Whole-cell lysates and tissue lysates from cells or the sample tissues were extracted by lysing the cells or the tissues in ice-cold RIPA buffer (Sevenbio, Beijing, China). 30 μg of total proteins were loaded per lane for western blotting analysis. Specific primary antibodies for WTAP (1:20000, 60188-1-Ig, Proteintech, China), CCND1 (1:20000, 26939-1-AP, Proteintech), RAF (1:1000, ab181115, Abcam, USA), RAF (phospho S259, 1:2500, ab173539, Abcam), MEK1/2 (1:1000, 11049-1-AP, Proteintech, China), MEK1/2 (phospho S221+S221, 0.1μg/ml, ab278564, Abcam), ERK1/2 (1:2000, 16443-1-AP, Proteintech), ERK1/2 (phospho T202+Y204, 0.075μg/ml, ab278538, Abcam) were used respectively. β-actin (1:2500, 20536-1-AP, Proteintech) and GAPDH (1:20000, 10494-1-AP, Proteintech) were used as loading controls.

Immunohistochemistry (IHC). Immunohistochemistry studies were performed by using the UltraSensitive TMSP (Mouse) IHC Kit (PV-9002, ZSGB-Bio, China) or Ultra-Sensitive TMSP (Rabbit) IHC Kit (PV-9001, ZSGB-Bio, China) according to the manufacturer's protocol. The tissue slides were steeped with xylene and 100% ethanol, followed by incubations in a series of decreased concentrations of ethanol. After antigen retrieval via autoclaving in pH 6.0 citrate buffer (Fuzhou Maixin Biotech), the slides were blocked and stained with a primary antibody WTAP (1:1000, 60188-1-Ig, Proteintech, China), CCND1 (1:1500, 26939-1-AP, Proteintech) or Ki-67 (1:5000, 27309-1-AP, Proteintech), followed by incubation with enhanced enzyme-labeled goat anti-mouse IgG polymer. Color development was performed by DAB (ZSGB-Bio, China), followed by hematoxylin treatment for counterstaining, after which they were dehydrated, and finally coverslipped. IHC score was evaluated according to a previously reported scoring method [39]. Staining intensities were described as 0 (negative), 1 (weak), 2 (moderate), or 3 (strongly positive). Percentages of positive areas were also scored. The intensity and extensity were summed up to determine the WTAP staining score for each patient.

MTS assay. To assess the proliferation ability, ESCC cells after transfection were seeded into 96-well plates with 1.0×10^3 cells/well, then Cell Titer 96®AQueous One Solution Reagent (Promega, USA) was adopted to each well to evaluate the proliferation at the point of 0, 24, 48, 72, and 96 h.

Colony formation assay. To further confirm the proliferation ability, transfected ESCC cells were replated into 6 well plates at a density of 1.0×10^3 cells/well. 10 days later, the cells were fixed by 4% formalin and stained with crystal violet solution for 30 min.

Wound healing assay. Transfected ESCC cells were seeded into 6-well culture plates until 100% confluent. Three vertical scratches were carefully produced by a sterile 200 μl pipette tip on the cultured cells. At 0 h and 24 h after the wound was created, a microscope was used to take photographs of the same scratched area to further calculate the relative distance of cell migration to the scratched area.

Migration and invasion assay. Migration assay was carried out by using transwell chambers (8 μm pore size, Corning Incorporated, USA). Transfected cells were added to the upper chamber at a density of 4×10^4/well in serum-free media, and a medium containing 20% FBS was added to the lower chamber. The invasion assay was similar to the migration assay with a pretreatment of 20 μl diluted Matrigel (BD Biosciences, USA) on the upper chambers. After 36 h incubation, the cells that did not invade the upper chamber were scraped and the invaded cells were stained with crystal violet solution and counted under a microscope.

mRNA-sequencing assay (mRNA-seq). KYSE150 cells of the logarithmic phase were transfected with siWTAP-1 or siNC for triplicate. 48 h incubation later, total RNA was extracted using TRIzol reagent (Invitrogen, USA), and the integrity of RNA was evaluated with Agilent 4150 (Agilent Technologies, USA). Then, mRNA-seq was performed on an Illumina Novaseq™ 6000 (Applied Protein Technology, China) according to the vendor's recommended protocol. StringTie and ballgown (http://bioconductor.org/packages/release/bioc/html/DESeq2.html) were adopted to the following analysis for the different expressions of all transcripts.

Animal experiments. The *in vivo* experiment scheme was approved by the Animal Care Committee of the Fourth Hospital of Hebei Medical University (IACUC Approval No.2023208). Eight 4-week-old male NOD-SCID mice were purchased from Beijing HFK Bioscience Co., Ltd. (Beijing, China) and were randomly divided into two groups. For the tumor formation assay, each mouse was subcutaneously inoculated with 1×10^7 KYSE150 in 200 μl PBS into the left flank. 5 days later, when the tumor nodules were 4 mm, the mice were injected with cholesterol-modified siWTAP-1 or siNC 10 nmol/mouse (RioBio, Guangzhou, China) intra-

tumorally with the frequency of once every 5 days. Before each injection, the tumor size and weight were measured. On the 25th day, the mice were sacrificed and xenografts were collected for the following detection of WTAP, CCND1, and Ki-67.

Statistical analysis. GraphPad Prism software 8.0 (San Diego, CA, USA) and SPSS software version 21.0 (Chicago, IL, USA) were used to create graphs and analyze results, respectively. Student's t-test was employed to calculate the measurement data and chi-square test was used to analyze the clinical data. Patients' prognosis was analyzed by the Kaplan-Meier method, and p-value less than or equal to 0.05 was considered statistically significant.

Results

WTAP was overexpressed in ESCC. Firstly, to clarify the potential role of WTAP in human ESCC, we explored the expression status of WTAP from the GEPIA dataset. The mRNA level of WTAP was significantly increased in ESCC compared to normal tissues (Figure 1A). Subsequently, we verified the different expression of WTAP by using the public TCGA dataset in ESCC, once again revealing that the mRNA expression level of WTAP was remarkably upregulated in ESCC malignancy compared to adjacent tissues (Figure 1B). To further illustrate the expression of WTAP in ESCC clinical samples, we next quantified the mRNA expression of the WTAP gene by qRT-PCR in 40 pairs of human ESCC tissues and matched adjacent tissues. Relative mRNA expression of WTAP was highly increased in ESCC tissues compared to the corresponding adjacent tissues (Figure 1C). Meanwhile, to validate the upregulated protein level of WTAP in ESCC samples, we carried out IHC staining and western blot in ESCC tissue and matched non-tumor tissues from the same donor. Figure 1D indicated that the staining pattern of WTAP in ESCC tissues was mostly nuclear, and the protein expression of WTAP was highly upregulated in ESCC malignancy based on the scoring of IHC results. In line with Figure 1D, Figure 1E confirmed that WTAP was highly overexpressed in ESCC tissues according to the quantification of western blot results.

To further clarify the function of WTAP in ESCC cell lines, we analyzed and compared the WTAP relative expression in 6 ESCC cell lines KYSE150, KYSE30, TE1, KYSE410, Eca109, and KYSE170. Figures 1F and 1G indicated that the expression of WTAP was higher in KYSE150 and KYSE30 cells and the expression of WTAP was lower in TE1 and KYSE410 cell lines. Based on this, in the following function research, WTAP expression was knocked down in KYSE150 and KYSE30 cells by transfection with siRNAs, and was overexpressed via transfection with the WTAP overexpression plasmid.

Table 1. Relevance of analysis of WTAP expression in ESCC patients.

WTAP Level Characteristics	n	Low	High	χ^2	p-value
Age (years)					
≤65	54	25	29	2.494	0.114
>65	54	17	37		
Gender					
Male	82	29	53	1.779	0.182
Female	26	13	13		
Lymph node metastasis					
Negative	50	25	25	4.837	0.028*
Positive	58	17	41		
Clinical stage					
I–II	50	23	27	8.946	0.159
III	58	19	39		
Pathological grade					
I–II	86	38	48	7.413	0.026*
III	22	4	18		
Tumor size (cm)					
≤4	43	20	23	6.408	0.186
>4	65	22	43		

Notes: A chi-square test was used for comparing groups between low and high WTAP expression; *p<0.05

WTAP was upregulated in human ESCC tissues and WTAP upregulation predicted a worse prognosis of ESCC patients. To uncover the relationship between WTAP expression and the survival of ESCC patients, an available chip array containing 108 ESCC tissues and 72 non-tumor adjacent tissues was selected to detect the WTAP expression by IHC. Based on the median IHC scoring, the 108 ESCC patients were divided into two groups: a group with WTAP high expression (n=66) and another group with WTAP low expression (n=42). Representative images of WTAP expression are shown in Figure 2A. The protein expression of WTAP in ESCC malignancy was upregulated when compared with that in non-tumor tissues, as shown in Figure 2B, identified by staining scores. Moreover, clinical data analysis suggested that patients with higher WTAP expression hold a poorer overall survival (Figure 2C). Furthermore, the elevated expression of WTAP in ESCC patients was significantly and positively correlated with lymph node metastasis and pathological grade (Table 1). These data suggest that WTAP upregulation was closely associated with ESCC progression and that WTAP may be used as a prognostic indicator for ESCC patients.

Knockdown of WTAP inhibited ESCC cell growth, migration, and invasion. To uncover the biological function of WTAP in ESCC cell lines, we downregulated the expression of WTAP under the force of siWTAPs in KYSE150 and KYSE30 cells. Firstly, the knockdown efficiency of siWTAP-1, siWTAP-2, and siWTAP-3 was evaluated in KYSE150 and KYSE30 cells by qRT-PCR. As shown in Supplementary Figure S1, after transfection of siWTAP-1, siWTAP-2, or siWTAP-3, the expression of WTAP in KYSE150 cells has been decreased to 20.2%, 21.2%, and 75.8%, and the expression of WTAP in KYSE30 cells has been decreased to 21.4%,

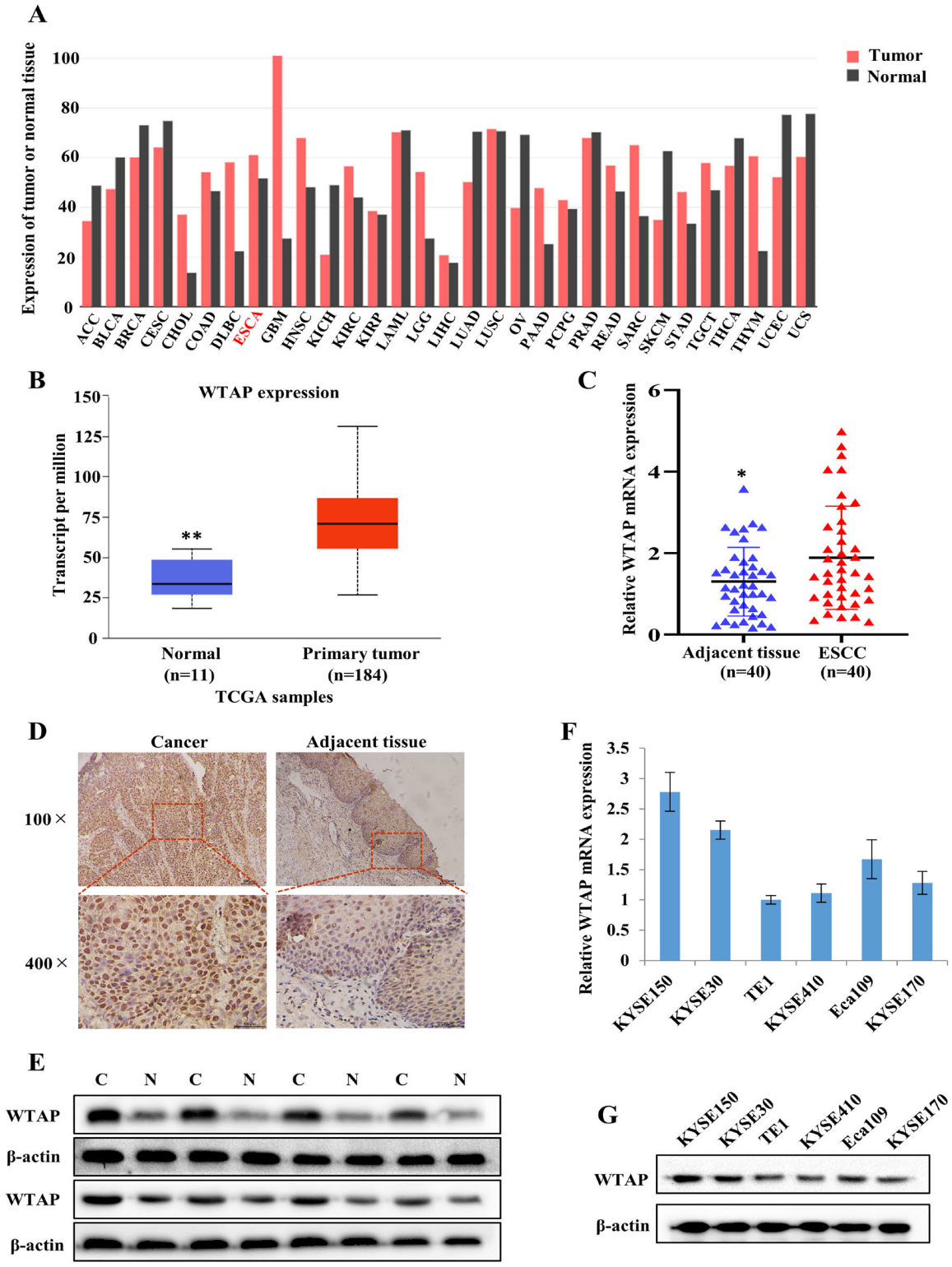

Figure 1. WTAP expression was upregulated in ESCC. A) The relative mRNA expression of WTAP in diverse cancers was determined based on the GEPIA datasets. B) The expression of WTAP mRNA in ESCC was determined based on TCGA datasets. C) The mRNA expression of WTAP was detected by qRT-PCR in 40 pairs of ESCC tissues. D) The expression of WTAP protein was analyzed by IHC in ESCC tissues and the matched adjacent tissues. E) The expression of WTAP protein was analyzed by western blotting in ESCC tissues and the matched adjacent normal tissues (C: Cancer; N: Normal). F, G) The relative expression of WTAP in 6 ESCC cell lines was detected by qRT-PCR and western blotting. *p<0.05, **p<0.01

25.0%, and 81.2%. Based on these results, in the following gain- and loss-of-function assays, we choose both siWTAP-1 and siWTAP-2 to silence WTAP.

In Figure 3A, an efficient knockdown of WTAP was confirmed via qRT-PCR and western blot assay. Growth curves plotted by MTS assay demonstrated that WTAP silence obviously inhibited KYSE150 and KYSE30 cell proliferation (Figure 3B). In addition, the growth ability of KYSE150 and KYSE30 cells was clearly decreased following WTAP knockdown, identified by smaller and fewer colonies in the WTAP silence group (Figure 3B). As shown in Figure 3C, the knockdown of WTAP by transfection with siWTAPs remarkably hindered the wound healing process compared to the control group. In addition, in both migration and invasion assays, the number of cells penetrating the membrane of the chambers was significantly lower in the WTAP silence group than in the control group (Figure 3D).

Overexpression of WTAP accelerated ESCC cell proliferation, invasion, and metastasis. To further investigate the potential functional role of WTAP in ESCC cells, we overexpressed WTAP by transfecting plasmid into TE1 and KYSE410 cells. Firstly, successful transfection of WTAP plasmid was verified at both mRNA and protein assays as shown in Figure 4A. As expected, transfection with WTAP significantly promoted the proliferation and colony formation abilities in TE1 and KYSE410 cells (Figure 4B). Furthermore,

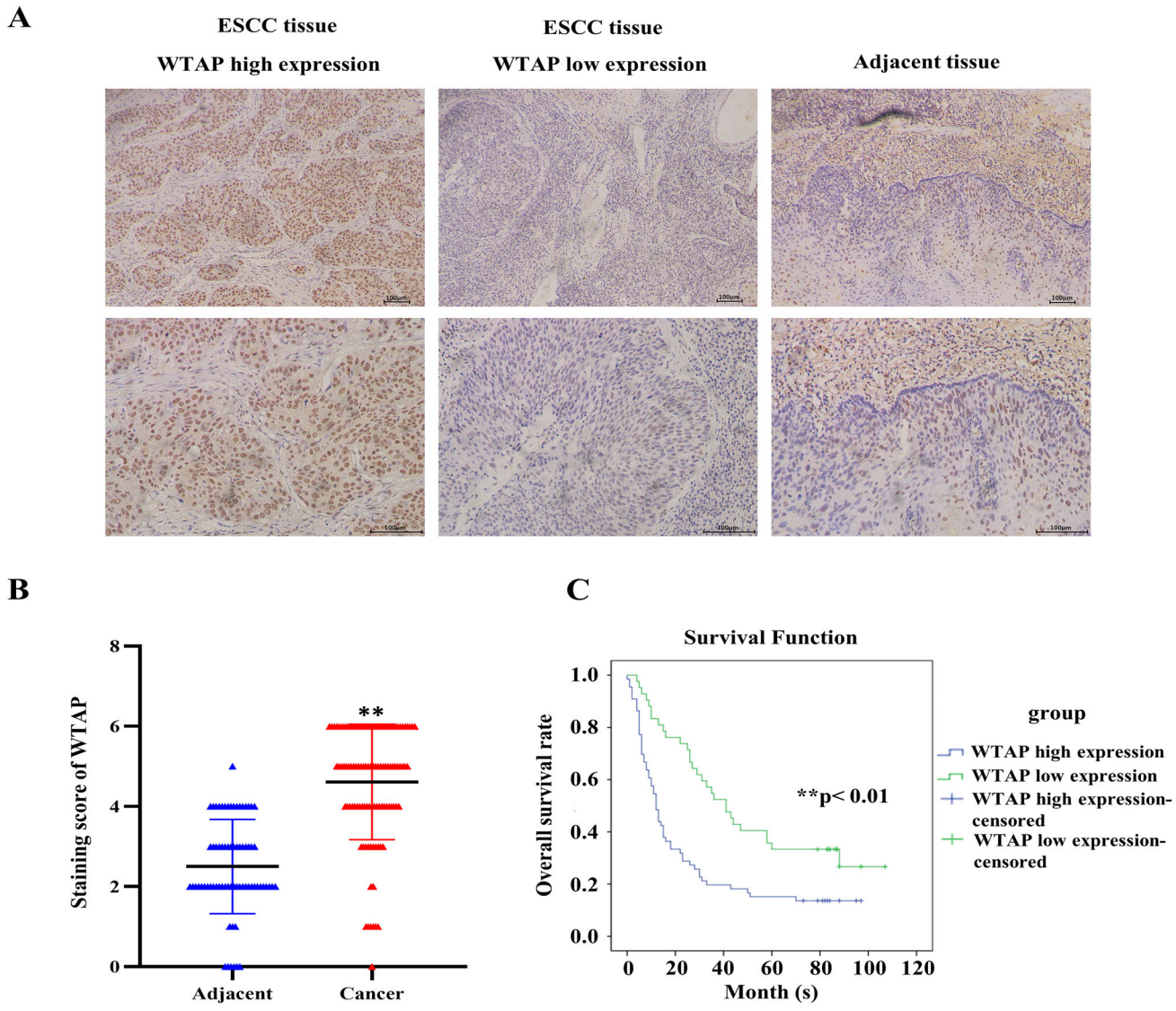

Figure 2. WTAP was upregulated in ESCC tissues and high expression predicted poor prognosis in ESCC patients. A) The representative images of WTAP expression in ESCC tissues and adjacent normal tissues by IHC assay. B) The relative protein expression of WTAP was analyzed by IHC in ESCC tissues and adjacent normal tissues quantified by scores. C) Kaplan-Meier analysis of overall survival (OS) of 108 ESCC patients was shown. **p<0.01

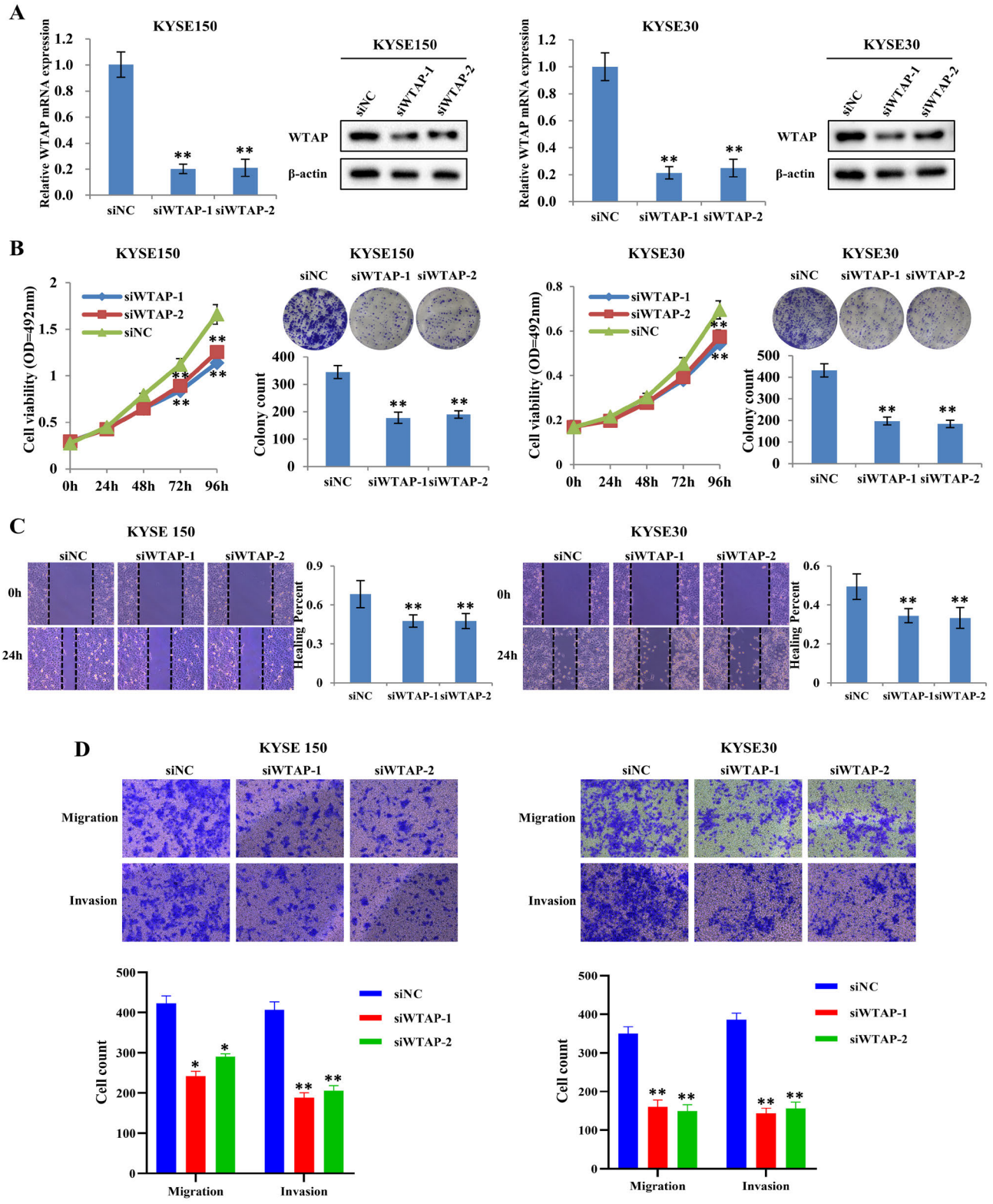

Figure 3. Knockdown of WTAP inhibited tumor growth and invasion of ESCC cells. A) Negative control or siRNA (siWTAP-1 and siWTAP-2) was transfected into KYSE150 and KYSE30 cells, respectively, and the knockdown efficiency was tested by qRT-PCR and western blotting. B) The proliferation capacities were detected by MTS and colony formation assay, with bar charts showing colony numbers. C, D) Effect of knocking down WTAP level was detected by scratching healing assay and Transwell assay. *p<0.05, **p<0.01

scratch wound healing assay and Transwell assay revealed that the overexpression of WTAP drastically facilitated the migrative and invasive capacity of TE1 and KYSE410 cells (Figures 4C, 4D). These data indicated that WTAP may play a tumorigenic role in promoting ESCC progression.

CCND1 was identified as the potential downstream target regulated by WTAP in ESCC. To ascertain the functional mechanism of WTAP and seek out its candidate downstream targets involved in ESCC progression, transcriptome sequencing was performed to probe into the expression difference in siWTAP-1 KYSE150 cells and control cells (Figure 5A). GO analysis suggested that differentially expressed genes were significantly enriched in gene clusters including cell developmental process, cell differentiation, multicellular organism development, and positive regulation of cell proliferation, indicating that WTAP could have a profound impact on the development and progression of ESCC (Figure 5B). Further analysis of the KEGG pathway revealed that 20 genes involved in the Mitogen-activated protein kinase (MAPK) signaling pathway were altered (Figure 5C). Next, 18 representative candidate genes (12 upregulated and 6 downregulated) were further confirmed by qRT-PCR, as shown in Figure 5D. Among the 18 genes, cyclin D1 (CCND1) was most significantly decreased in KYSE150 and KYSE30 cells with depletion of WTAP, compared with that in the control cells. Next, we validated CCND1 upregulation in ESCC tissues using qRT-PCR in 40 pairs of ESCC and their corresponding tissues, and the results showed that CCND1 expression was significantly increased in ESCC tissues compared with that in the matched adjacent tissues (Figure 5E).

To further verify whether CCND1 and MAPK signaling pathway were involved in the progression of ESCC induced by WTAP, we performed a western blot to determine the expression of CCND1 and MAPK-related molecules. As respected, the expression of WTAP, CCND1, p-RAF, p-MEK, and p-ERK were dramatically suppressed, while the expression of RAF, MEK, and ERK was not changed when WTAP was silenced in both KYSE150 and KYSE30 cells (Figure 5F). Correspondingly, after the overexpression of WTAP, the expression levels of WTAP, CCND1, p-RAF, p-MEK, and p-ERK in ESCC cells were remarkably increased compared to the control cells, whereas RAF, MEK, and ERK were not changed (Figure 5F). These findings confirmed the ability of WTAP to regulate the proliferation and metastasis of ESCC via phosphorylating the MAPK signaling pathway by regulating the downstream target CCND1.

Overexpression of CCND1 reversed the effects of siWTAP in ESCC. To further make sure that CCND1 participated in the effects of WTAP on ESCC progression, we conducted a series of rescue assays. In these rescue assays, we reintroduced CCND1 expression by transfecting the overexpression plasmid in WTAP-silenced KYSE150 and KYSE30 cells. Results indicated that the overexpression CCND1 group could partially rescue the decreased proliferation and clone formation ability of KYSE150 and KYSE30 cells caused by WTAP depletion (Figures 6A, 6B). Additionally, the overexpressed CCND1 group partially promoted the decreased ability of the migration and invasion that was induced by WTAP knockdown (Figures 6C, 6D). In Figure 6E, the decreased expression of p-RAF, p-MEK, and p-ERK in KYSE150 and KYSE30 cells by silencing of WTAP was rescued due to forced expression of CCND1. Therefore, our results verified that CCND1 was a main downstream medium participating in the upregulated proliferation and metastatic activity of ESCC induced by WTAP via phosphorylation of the MAPK signaling pathway.

WTAP promoted ESCC cell growth *in vivo*. In order to investigate the carcinogenic function of WTAP in ESCC cells *in vivo*, we tested the tumorigenicity of KYSE150 cells by subcutaneous implanting KYSE150 cells followed by intratumoral injecting cholesterol-modified siWTAP-1 or siNC in 4-week nude mice, and 25 days later the mice were killed for tumor resection (Figure 7A). Compared with the siNC group, intratumoral siWTAP-1 injection significantly inhibited the subcutaneous xenograft growth, including tumor size and tumor weight (Figures 7B–7D). The relative mRNA expression of WTAP and CCND1 in the WTAP-silenced xenograft tumors was significantly decreased compared to the NC groups (Figures 7E, 7F). Histologic analysis indicated that xenografted tumors from the siWTAP-1 groups showed decreased intensity and extensity of WTAP, CCND1, and Ki-67 compared to the siNC groups (Figure 7G). Taken together, our results suggest that WTAP and CCND1 play a pivotal role in promoting ESCC growth.

Discussion

m6A, as a pervasive internal mRNA modification, was extensively investigated in the progression of cancers. Recently, accumulating evidence has hinted at the potential roles of m6A regulators, especially the writer complex of METTL3, METTL14, and WTAP. In this research, we focused on the effect of WTAP and its potential mechanism in the WTAP-dependent progression and metastasis of ESCC.

Emerging evidences indicated that WTAP plays a critical role in cancer development [21–32]. Chen et al. [27] reported that WTAP is remarkably upregulated in hepatocellular carcinoma and facilitates liver cancer malignant progression via theHuR-ETS1-p21/p27 axis. Chen et al. [28] identified elevated expression of WTAP is associated with poor prognosis in osteosarcoma patients by an underlying mechanism of regulating HMBOX1 mRNA stability via PI3K/AKT pathway to affect osteosarcoma growth and metastasis. Similar reports have also been found in gastric cancer, acute myelogenous leukemia, colorectal cancer, glioblastoma, renal cell carcinoma, glioma, bladder cancer, pancreatic cancer, lymphoma, and cholangiocarcinoma [21–26, 29–32]. Consistent with the previous findings, we reported for the

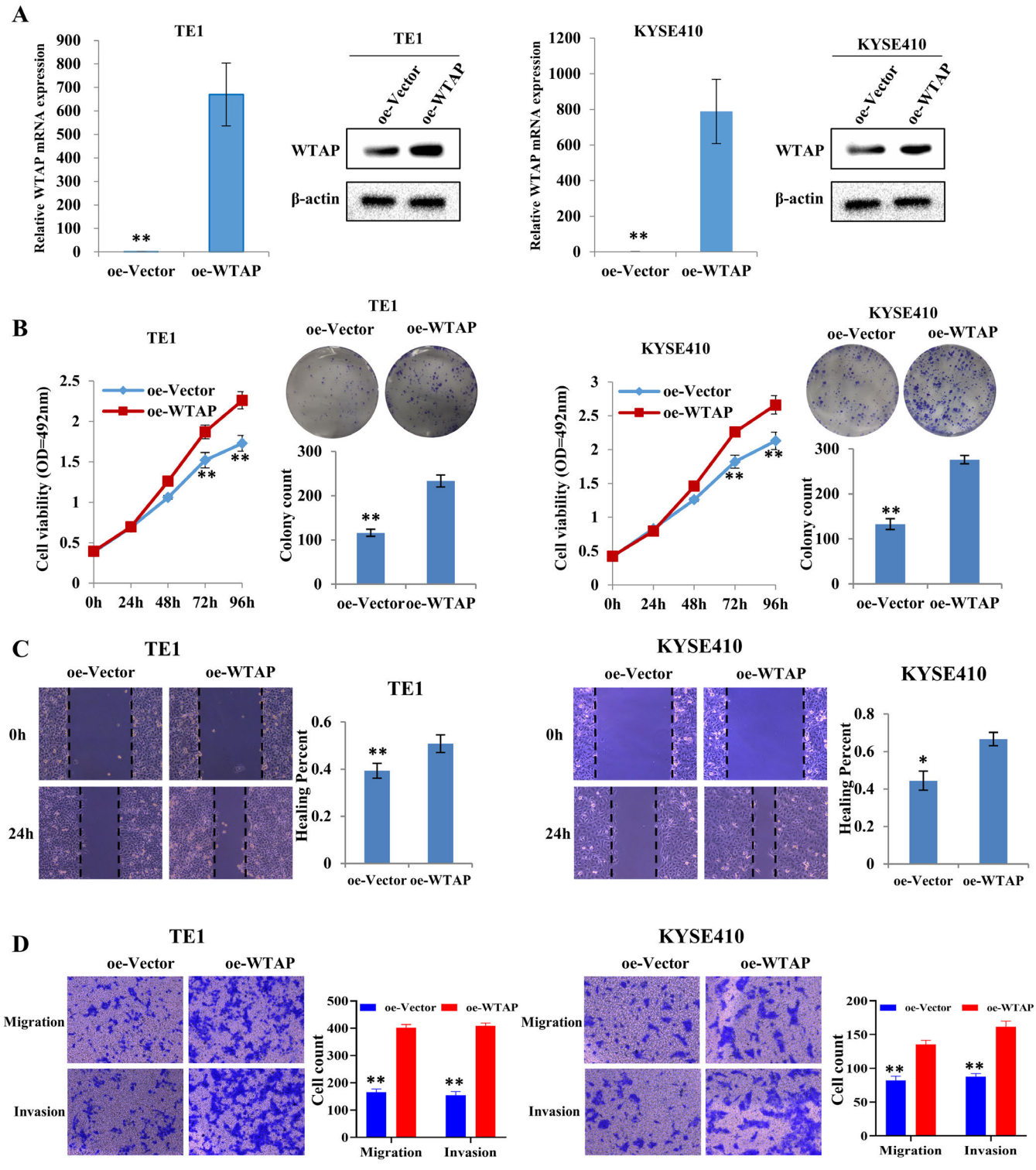

Figure 4. Overexpression of WTAP facilitated ESCC cell proliferation and migration. A) The overexpression effect was verified at the mRNA level using qRT-PCR and protein level using western blot. B) MTS and colony formation assay showed that overexpression of WTAP promoted ESCC cell proliferation. C, D) Wound healing assay and Transwell assay revealed that overexpression of WTAP significantly accelerated ESCC cell migration. *p<0.05, **p<0.01

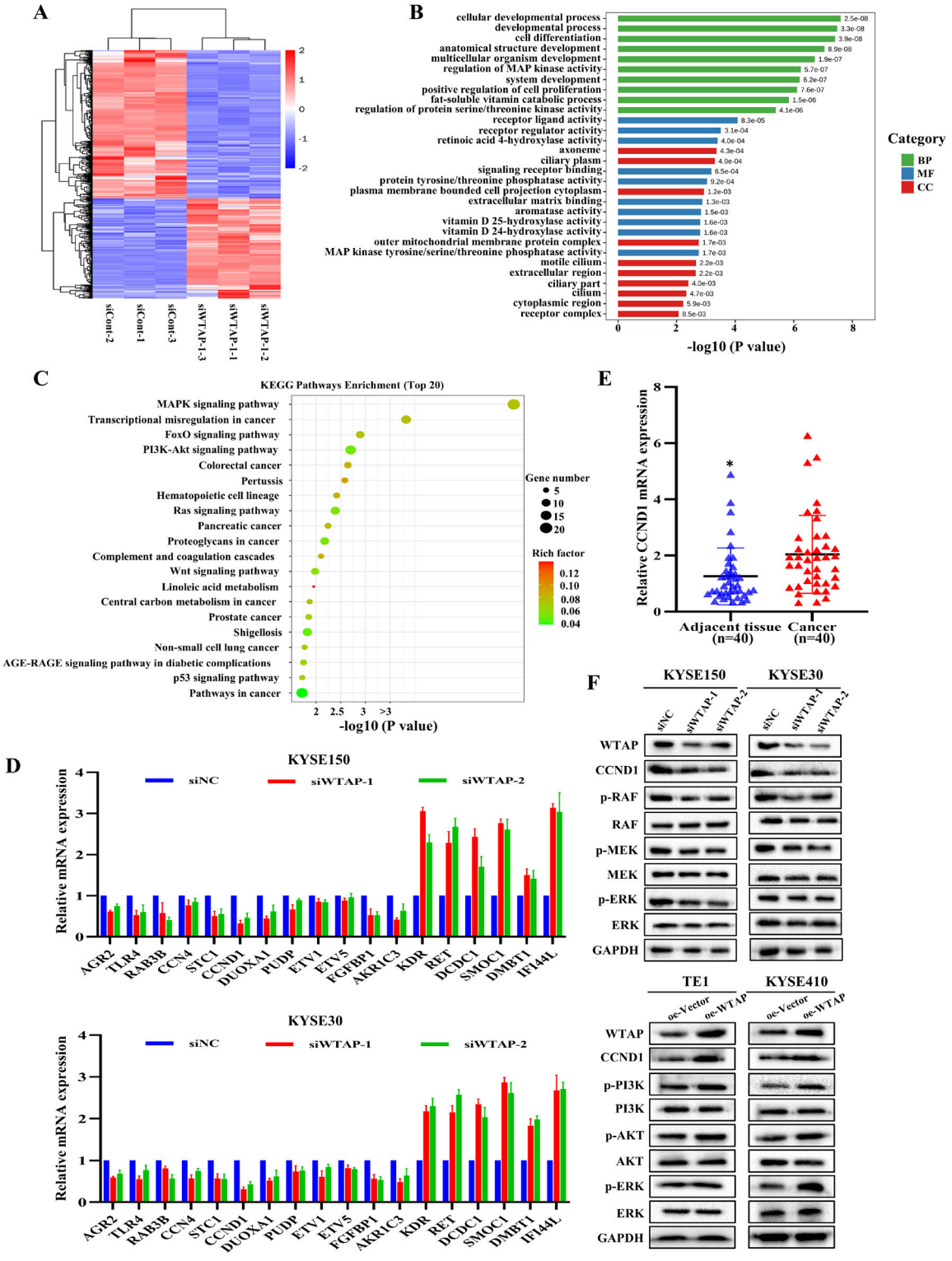

Figure 5. CCND1 and MAPK pathway were proved to be involved in WTAP-mediated ESCC progression. A) Different genes in KYSE150 cells treated with siWTAP-1 and siNC were identified by mRNA-seq. The screening criteria were the fold change value of upregulation or downregulation <2 and the p-value <0.05. B, C) Enrichment analysis for representative GO analysis and KEGG pathways in WTAP target genes. D) Relative mRNA expression levels of representative genes in KYSE150 cells and KYSE30 cells treated with siWTAP-1 compared with that in the control cells. E) The mRNA expression of CCND1 was detected by qRT-PCR in 40 pairs of ESCC tissues. F) The protein expression of WTAP, CCND1, and MAPK-related molecules RAF, MEK, ERK were assessed by western blot. *p<0.05

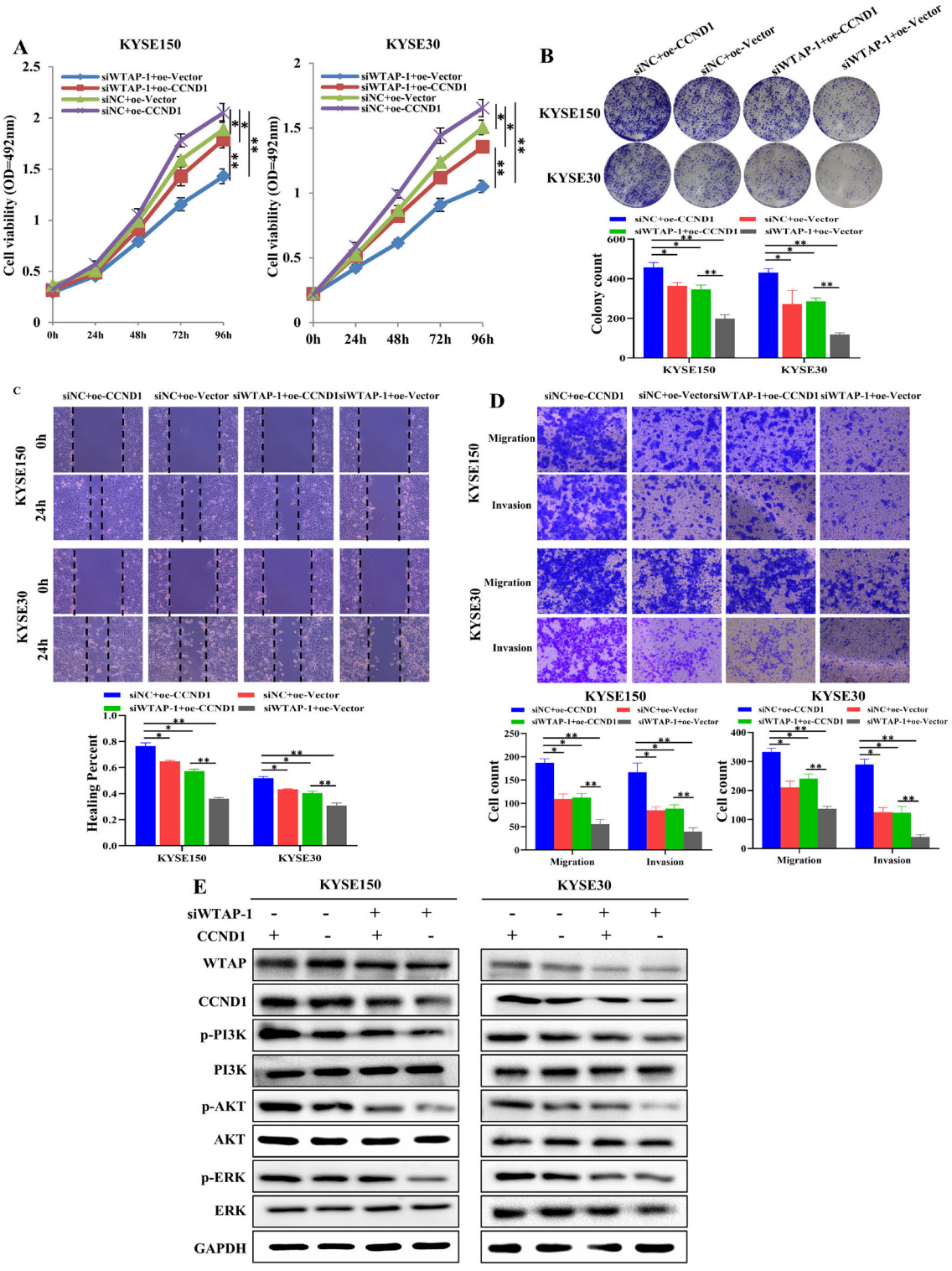

Figure 6. CCND1 reversed the effects of siWTAP-1 on the proliferation, migration, and invasion of ESCC cells. A, B) The siNC+oe-CCND1 group increased the proliferation and clone formation of ESCC compared with the siNC+oe-Vector group, and the siWTAP-1+oe-CCND1 group also facilitated the proliferation and clone formation of ESCC compared with the siWTAP-1+oe-Vector group. C, D) The siNC+oe-CCND1 group promoted the migration and invasion of ESCC compared with the siNC+oe-Vector group, and the siWTAP-1+oe-CCND1 group rescued the migration and invasion of ESCC compared with the siWTAP-1+oe-Vector group. E) The siNC+oe-CCND1 group accelerated phosphorylation status of the MAPK pathway-related molecules such as RAF, MEK, ERK in ESCC cells compared with the siNC+oe-Vector group, and the siWTAP-1+oe-CCND1 group also promoted phosphorylation status of RAF, MEK, ERK compared with the siWTAP-1+oe-Vector group. *p<0.05, **p<0.01

first time that WTAP was markedly upregulated in ESCC tissues, and that elevated WTAP expression was positively relevant with lymph node metastasis, pathological grade, and a worse clinical prognosis. In addition, we probed into the biological effect of WTAP in ESCC cell lines, and the results suggested that the knockdown of WTAP significantly inhibited ESCC cell growth and invasion. Furthermore, the overexpression of WTAP significantly facilitated the proliferation, migration, and invasion of ESCC cells. Moreover, the subcutaneous implantation experiment confirmed that WTAP knockdown inhibited the growth of ESCC cells *in vivo*. These data indicated that WTAP might function as an oncogenic protein in ESCC development and might be considered to be a potential therapeutic target. However, the underlying tumorigenic mechanism of WTAP in ESCC progression remains obscure.

A previous study demonstrated that WTAP regulated the migration and invasion of cholangiocarcinoma cells by inducing the expressions of some oncogenes, such as MMP7, MMP28, cathepsin H, and Muc1 [32]. Moreover, Tang et al. [25] indicated that WTAP promoted renal carcinoma growth via strengthening the cyclin-dependent kinases 2 (CDK2) mRNA stability. Furthermore, Chen et al. [27] reported that WTAP regulated the G2/M phase of

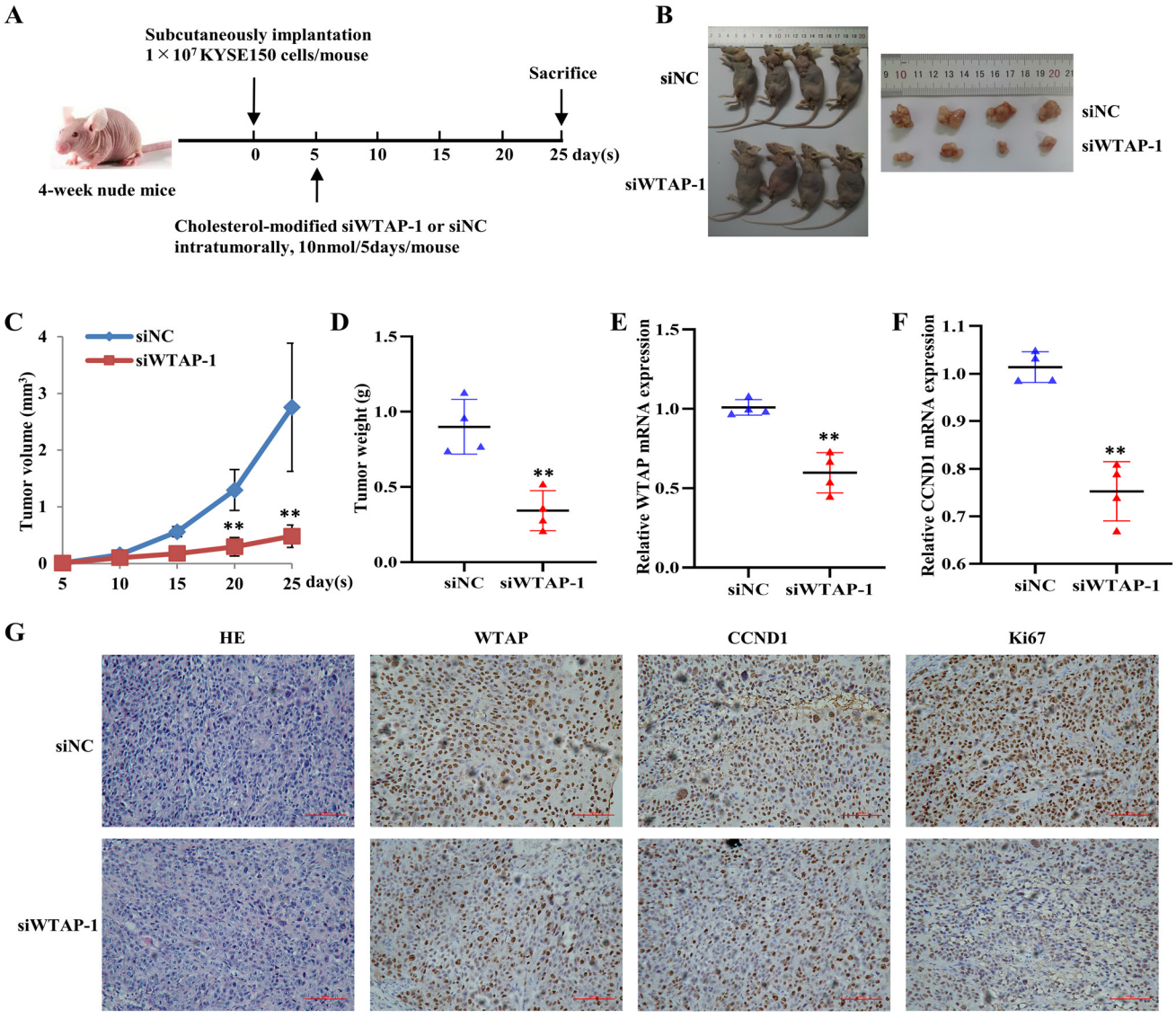

Figure 7. WTAP interacted with CCND1 and promoted ESCC growth *in vivo*. A) Schematic diagram of grouping for xenotransplantation model. B) Images of nude mice and xenografts in the indicated groups. C, D) The volume (C) and weight (D) of subcutaneous xenograft tumors. E, F) The relative mRNA expression of WTAP and CCND1 in xenograft tumors of the tsiWTAP-1 group and the control group. G) The representative immunohistochemical images of WTAP, CCND1, and Ki-67 in xenografted tumors from the siWTAP-1 group and the siNC group. **p<0.01

hepatocellular carcinoma cells by suppressing the biological function of ETS1. While, in our present study, we performed an mRNA-seq analysis using KYSE150 cells silenced by siWTAP-1 and siNC, and collected 18 representative candidate genes (12 upregulated and 6 downregulated). After further qRT-PCR confirmation, CCND1 was identified as a potential downstream of WTAP in the progression of ESCC. Furthermore, through KEGG analysis, the MAPK pathway which enriched the most differential genes was regarded as the most important involved pathway in WTAP-mediated ESCC progression.

CCND1, the most famous member belonging to the D-type cyclin proteins family, was considered a critical element regulating cell cycle progression [33]. Cell cycle processes are driven by complexes consisting of a series of different cyclins and CDKs. Under the fine modulation of cyclin/CDKs, cells can accurately regulate the cell cycle to ensure normal growth and metabolism. As we know, the cyclin D family consists of D1, D2, and D3, which could sense signaling stimuli inside and outside of the cells, and then bind to and activate CDK4/6, to further modulate the cell cycle [40]. Furthermore, due to its broad involvement in cellular functions, CCND1 has been considered the most dominant member among the cyclin D family. Abnormal expression of CCND1 in the initial stage of a malignant tumor can lead to chromosome rearrangement and abnormal gene amplification, identifying that CCND1 may play an important role in the process of carcinogenesis [34–36]. In our present study, CCND1 was confirmed to regulate the development of ESCC as the key downstream target of WTAP. Further qRT-PCR results demonstrated that the mRNA expression of CCND1 was upregulated in ESCC malignancy compared to the adjacent non-tumor tissues from the same donors, and western blot analysis showed that the protein expression of CCND1 could be downregulated by the WTAP knockdown in ESCC cell lines. The overexpression of CCND1 rescued the decreased cell proliferation, colony formation, and cell migration forced by the silence of WTAP in ESCC cells. All of these suggested that CCND1 also plays a crucial oncogene role in the carcinogenesis of ESCC. Moreover, in our research, we verified that WTAP accelerates ESCC progression by upregulating the expression of CCND1, which was consistent with previous reports that WTAP participated in carcinogenesis by regulating cyclins or CDKs [25, 27].

The MAPK pathway is the most dysregulated pathway involved in many cancers including ESCC [37]. Based on the KEGG analysis from our mRNA-seq, the MAPK pathway enriched the most 20 differential genes, so as to be regarded as the most important involved pathway in WTAP-dependent ESCC progression. Moreover, the phosphorylation status of the MAPK pathway-related molecules such as RAF, MEK, ERK was verified to be strengthened in the WTAP overexpression group and to be impaired in the WTAP silenced group, which further confirmed our hypothesis that MAPK was involved in WTAP-promoted ESCC progression.

In summary, we showed that WTAP promotes ESCC tumorigenesis by regulating the downstream target oncogene CCND1, via activating the phosphorylation of MAPK pathway molecules. We concluded that WTAP may be a candidate prognostic biomarker for ESCC and targeting the WTAP-CCND1 axis will be a promising strategy for ESCC cancer therapy.

Supplementary information is available in the online version of the paper.

Acknowledgments: The present study was supported by the Natural Science Foundation of China (Grant No. U21A20415).

References

[1] SIEGEL RL, MILLER KD, FUCHS HE, JEMAL A. Cancer statistics, 2022. CA Cancer J Clin 2022; 72: 7–33. https://doi.org/10.3322/caac.21708

[2] BRAY F, FERLAY J, SOERJOMATARAM I, SIEGEL RL, TORRE LA et al. Global cancer statistics 2018: GLOBOCAN estimates of incidence and mortality worldwide for 36 cancers in 185 countries. CA Cancer J Clin 2018; 68: 394–424. https://doi.org/10.3322/caac.21492

[3] CHEN W, ZHENG R, BAADE PD, ZHANG S, ZENG H et al. Cancer statistics in China, 2015. CA Cancer J Clin 2016; 66: 115–132. https://doi.org/org/10.3322/caac.21338

[4] MORGAN E, SOERJOMATARAM I, GAVIN AT, RUTHERFORD MJ, GATENBY P et al. International trends in oesophageal cancer survival by histological subtype between 1995 and 2014. Gut 2021; 70: 234–242. https://doi.org/10.1136/gutjnl-2020-321089

[5] FU Y, DOMINISSINI D, RECHAVI G, HE C. Gene expression regulation mediated through reversible m(6)A RNA methylation. Nat Rev Genet 2014; 15: 293–306. https://doi.org/10.1038/nrg3724

[6] WANG X, LU Z, GOMEZ A, HON GC, YUE Y et al. N6-methyladenosine-dependent regulation of messenger RNA stability. Nature 2014; 505: 117–120. https://doi.org/10.1038/nature12730

[7] XIAO W, ADHIKARI S, DAHAL U, CHEN YS, HAO YJ et al. Nuclear m6a reader YTHDC1 regulates mRNA splicing. Mol Cell 2016; 61: 507–519. https://doi.org/10.1016/j.molcel.2016.01.012

[8] MEYER KD, PATIL DP, ZHOU J, ZINOVIEV A, SKABKIN MA et al. 5' UTR m(6)A promotes cap-independent translation. Cell 2015; 163: 999–1010. https://doi.org/10.1016/j.cell.2015.10.012

[9] WANG X, ZHAO BS, ROUNDTREE IA, LU Z, HAN D et al. N(6)-methyladenosine modulates messenger RNA translation efficiency. Cell 2015; 61: 1388–1399. https://doi.org/10.1016/j.cell.2015.05.014

[10] DENG X, SU R, FENG X, WEI M, CHEN J. Role of N(6)-methyladenosine modification in cancer. Curr Opin Genet Dev 2017; 48: 1–7. https://doi.org/org/10.1016/j.gde.2017.10.005

[11] BOKAR JA, SHAMBAUGH ME, POLAYES D, MATERA AG, ROTTMAN FM. Purification and cDNA cloning of the AdoMet-binding subunit of the human mRNA (N6-adenosine)-methyltransferase. RNA 1997; 3: 1233–1247.
[12] LIU J, YUE Y, HAN D, WANG X, FU Y et al. A METTL3-METTL14 complex mediates mammalian nuclear RNA N6-adenosine methylation. Nat Chem Biol 2014; 10: 93–95. https://doi.org/10.1038/nchembio.1432
[13] PING XL, SUN BF, WANG L, XIAO W, YANG X et al. Mammalian WTAP is a regulatory subunit of the RNA N6-methyladenosine methyltransferase. Cell Res 2014; 24: 177–189. https://doi.org/10.1038/cr.2014.3
[14] WANG Y, LI Y, TOTH JI, PETROSKI MD, ZHANG Z et al. N6-methyladenosine modification destabilizes developmental regulators in embryonic stem cells. Nat Cell Biol 2014b; 16: 191–198. https://doi.org/10.1038/ncb2902
[15] WANG X, FENG J, XUE Y, GUAN Z, ZHANG D et al. Structural basis of N(6)-adenosine methylation by the METTL3-METTL14 complex. Nature 2016; 534: 575–578. https://doi.org/10.1038/nature18298
[16] LITTLE NA, HASTIE ND, DAVIES RC, HASTIE ND, DAVIES RC. Identification of WTAP, a novel Wilms' tumour 1-associating protein. Hum Mol Genet 2000; 9: 2231–2239. https://doi.org/10.1093/oxfordjournals.hmg.a018914
[17] ORTEGA A, NIKSIC M, BACHI A, WILM M, SANCHEZ L et al. Biochemical function of female-lethal (2)D/Wilms' tumor suppressor-1-associated proteins in alternative pre-mRNA splicing. J Biol Chem 2003; 278: 3040–3047. https://doi.org/10.1074/jbc.M210737200
[18] CHIE N, YOSHIYASU F, DAI K, MASAHIDE A. A novel gene trapping for identifying genes expressed under the control of specific transcription factors. Biochem Biophys Res Commun 2007; 361: 109–115. https://doi.org/10.1016/j.bbrc.2007.06.161
[19] HORIUCHI K, UMETANI M, MINAMI T, OKAYAMA H, TAKADA S et al. Wilms' tumor 1-associating protein regulates G2/M transition through stabilization of cyclin A2 mRNA. Proc Natl Acad Sci U S A 2006; 103: 17278–17283. https://doi.org/10.1073/pnas.0608357103
[20] XIE W, WEI L, GUO J, GUO H, SONG X et al. Physiological functions of Wilms' tumor 1-associating protein and its role in tumourigenesis. J Cellular Biochem 2019; 120: 10884–10892. https://doi.org/10.1002/jcb.28402
[21] YU H, ZHAO K, ZENG H, LI Z, CHEN K et al. N-methyladenosine (mA) methyltransferase WTAP accelerates the Warburg effect of gastric cancer through regulating HK2 stability. Biomed Pharmacother 2021; 133: 111075. https://doi.org/10.1016/j.biopha.2020.111075
[22] NAREN D, YAN T, GONG Y, HUANG J, ZHANG D et al. High Wilms' tumor 1 associating protein expression predicts poor prognosis in acute myeloid leukemia and regulates m(6)A methylation of MYC mRNA. J Cancer Res Clin Oncol 2021; 147: 33–47. https://doi.org/10.1007/s00432-020-03373-w
[23] ZHANG J, TSOI H, LI X, WANG H, GAO J et al. Carbonic anhydrase IV inhibits colon cancer development by inhibiting WNT signaling pathway through targeting WTAP-WT1-TBL1 Axis. Gut 2015; 13: e78–e79. https://doi.org/10.1136/gutjnl-2014-308614
[24] JIN DI, LEE SW, HAN ME, KIM HJ, SEO SA et al. Expression and roles of Wilms' tumor 1-associating protein in glioblastoma. Cancer Sci 2012; 103: 2102–2109. https://doi.org/10.1111/cas.12022
[25] TANG J, WANG F, CHENG G, SI S, SUN X et al. Wilms' tumor 1-associating protein promotes renal cell carcinoma proliferation by regulating CDK2 mRNA stability. J Exp Clin Cancer Res 2018; 37: 40. https://doi.org/10.1186/s13046-018-0706-6
[26] XI Z, XUE Y, ZHENG J, LIU X, MA J et al. WTAP Expression Predicts Poor Prognosis in Malignant Glioma Patients. J Mol Neurosci 2016; 60: 1–6. https://doi.org/10.1007/s12031-016-0788-6
[27] CHEN Y, PENG C, CHEN J, CHEN D, YANG B et al. WTAP facilitates progression of hepatocellular carcinoma via m6A-HuR-dependent epigenetic silencing of ETS1. Mol Cancer 2019; 18: 127. https://doi.org/10.1186/s12943-019-1053-8
[28] CHEN S, LI Y, ZHI S, DING Z, WANG W et al. WTAP promotes osteosarcoma tumorigenesis by repressing HMBOX1 expression in an m6A-dependent manner. Cell Death Dis 2020; 11: 659. https://doi.org/10.1038/s41419-020-02847-6
[29] WANG K, WANG G, LI G, ZHANG W, WANG Y et al. m6A writer WTAP targets NRF2 to accelerate bladder cancer malignancy via m6A-dependent ferroptosis regulation. Apoptosis 2023; 28: 627–638. https://doi.org/10.1007/s10495-023-01817-5
[30] DENG J, ZHANG J, YE Y, LIU K, ZENG L et al. N6-methyladenosine-Mediated Upregulation of WTAPP1 Promotes WTAP Translation and Wnt Signaling to Facilitate Pancreatic Cancer Progression. Cancer Res 2021; 81: 5268–5283. https://doi.org/10.1158/0008-5472.CAN-21-0494
[31] KUAI Y, GONG X, DING L, LI F, LEI L et al. Wilms' tumor 1-associating protein plays an aggressive role in diffuse large B-cell lymphoma and forms a complex with BCL6 via Hsp90. Cell Commun Signal 2018; 16: 50. https://doi.org/10.1186/s12964-018-0258-6
[32] JO HJ, SHIM HE, HAN ME, KIM HJ, KIM KS et al. WTAP regulates migration and invasion of cholangiocarcinoma cells. J Gastroenterol 2013; 48: 1271–1282. https://doi.org/10.1007/s00535-013-0748-7
[33] QIE S, DIEHL JA. Cyclin D1, cancer progression, and opportunities in cancer treatment. J Mol Med (Berl) 2016; 94: 1313–1326. https://doi.org/10.1007/s00109-016-1475-3
[34] AI B, KONG X, WANG X, ZHANG K, YANG X et al. LINC01355 suppresses breast cancer growth through FOXO3-mediated transcriptional repression of CCND1. Cell Death Dis 2019; 10: 502. https://doi.org/10.1038/s41419-019-1741-8
[35] ZHENG L, LIANG X, LI S, LI T, SHANG W et al. CHAF1A interacts with TCF4 to promote gastric carcinogenesis via upregulation of c-MYC and CCND1 expression. EBioMed 2018; 38: 69–78. https://doi.org/10.1016/j.ebiom.2018.11.009
[36] WANG M, YU W, GAO J, MA W, FRENTSCH M et al. MicroRNA-487a-3p functions as a new tumor suppressor in prostate cancer by targeting CCND1. J Cell Physiol 2020; 235: 1588–1600. https://doi.org/10.1002/jcp.29078

[37] LI R, ZENG L, ZHAO H, DENG J, PAN L et al. ATXN2-mediated translation of TNFR1 promotes esophageal squamous cell carcinoma via m6A-dependent manner. Mol Ther 2022; 30: 1089–1103. https://doi.org/10.1016/j.ymthe.2022.01.006

[38] LIVAK KJ, SCHMITTGEN TD. Analysis of relative gene expression data using real-time quantitative PCR and the 2(-Delta Delta C(T)) method. Methods 2001; 25: 402–408. https://doi.org/10.1006/meth.2001.1262

[39] YOKOYAMA Y, SATO S, FUTAGAMI M, FUKUSHI Y, SAKAMOTO T et al. Prognostic significance of vascular endothelial growth factor and its receptors in endometrial carcinoma. Gynecol Oncol 2000; 77: 413–418. https://doi.org/10.1006/gyno.2000.5802

[40] VANARSDALE T, BOSHOFF C, ARNDT KT, ABRAHAM RT. Molecular pathways: targeting the cyclin D–CDK4/6 axis for cancer treatment. Clin Cancer Res 2015; 21: 2905. https://doi.org/10.1158/1078-0432.CCR-14-0816

https://doi.org/10.4149/neo_2024_231219N653

WTAP/CCND1 axis accelerates esophageal squamous cell carcinoma progression by MAPK signaling pathway

Hong ZHANG[1], Xiaojing ZHANG[2], Yan ZHANG[3], Jianhua WU[4], Jiali LI[1,*], Baoen SHAN[1,*]

Supplementary Information

Supplementary Table S1. Primer sequences and reaction conditions.

Gene	Primer sequence	Annealing temperature	Product size, bp
AGR2	F: 5'- AGAGCAGTTTGTCCTCCTCAA -3' R: 5'- CAGGTTCGTAAGCATAGAGA-3'	55 °C	161
AKR1C3	F: 5' - ACGATGGGTGGACCCGAA -3' R: 5'- CGTTCTGTCTGATGCGCTGC -3'	59 °C	167
WTAP	F: 5'-TTCCCAAGAAGGTTCGATTG-3' R: 5'-TGCAGACTCCTGCTGTTGTT-3'	57 °C	192
CCND1	F: 5'- AGCTGTGCATCTACACCGAC -3' R: 5'- GAAATCGTGCGGGGTCATTG -3'	59 °C	113
DUOXA1	F: 5'- CATTCCTCTGCTGGCTACTG -3' R: 5'- AGCATGTGGCCACCATAAAC -3'	57 °C	91
FGF1	F:5'- CTTCACAGCAAAGTGGTCTCA -3' R: 5'- GACACAGGAAAATTCATGGTCCA -3'	57 °C	195
PUDP	F: 5'- GCAATGACAACTGATAAAGCGAGATG -3' R: 5'- GCTAACAAGGAGTGCTCATCAAAAAC -3'	55 °C	146
RAB3B	F: 5'- CGGGTGAAACTGCAGATCT -3' R: 5'- CTGAGTAGCCCAGTCTTGGA -3'	56 °C	150
TLR4	F: 5'- TGGTGTGTCGGTCCTCAGTGTG -3' R: 5'- AGCCAGCAAGAAGCATCAGGTG -3'	57 °C	89
DMBT1	F: 5'- ACACATTGCCGACCATCACCTTG-3' R: 5'- TCACCTCCATTCACCAGCCTCAG-3'	56 °C	119
ETV1	F: 5'- CATCGCAGTCCATACCAGATAGCAG-3' R: 5'- CATCGTCGGCAAAGGAGGAAAGG-3'	57 °C	128
ETV5	F: 5'- GTGTTGTGCCTGAGAGACTGGAAG-3' R: 5'- CATTGGCTGGGTCATCAAGAAGGG-3'	56 °C	135
CCN4	F: 5'- GGAAGAAGTGTCTGGCTGTGTACC-3' R: 5'- GTACTTGGGTTGATAGGAGCGTGTG-3'	57 °C	92
STC1	F: 5'- CCATGAGGCGGAGCAGAATGAC-3' R: 5'- GCCGACCTGTAGAGCACTGTTG-3'	59 °C	106
SMOC1	F: 5'- TGTGACCAGGAGAGGCAGAGTG-3' R: 5'- CACCAGCACACACCAGCAGTAG-3'	60 °C	144
RET	F: 5'- AAGAGACGGCTGGAGTGTGAGG-3' R: 5'- TGGGAGAGCAGGTGGAGAAGTTC-3'	51 °C	115
KDR	F: 5'- AGGGAGTCTGTGGCATCTGAAGG-3' R: 5'- GTGGTGTCTGTGTCATCGGAGTG-3'	59 °C	80
IFI44L	F: 5'- CACCAGCATAACCGAGCGGTATAG-3' R: 5'- TTCTGCCCCATCTAGCCCCATAG-3'	61 °C	99
DCDC1	F: 5'- CAGTGAAGCAAGCAGCAGGAGTC-3' R: 5'- GTTATCGCTCGGCTCAGGATCATTC-3'	58 °C	149
GAPDH	F: 5'-AATCCCATCACCATCTTCCA-3' R: 5'-TGGACTCCACGACGTACTCA -3'	57 °C	82

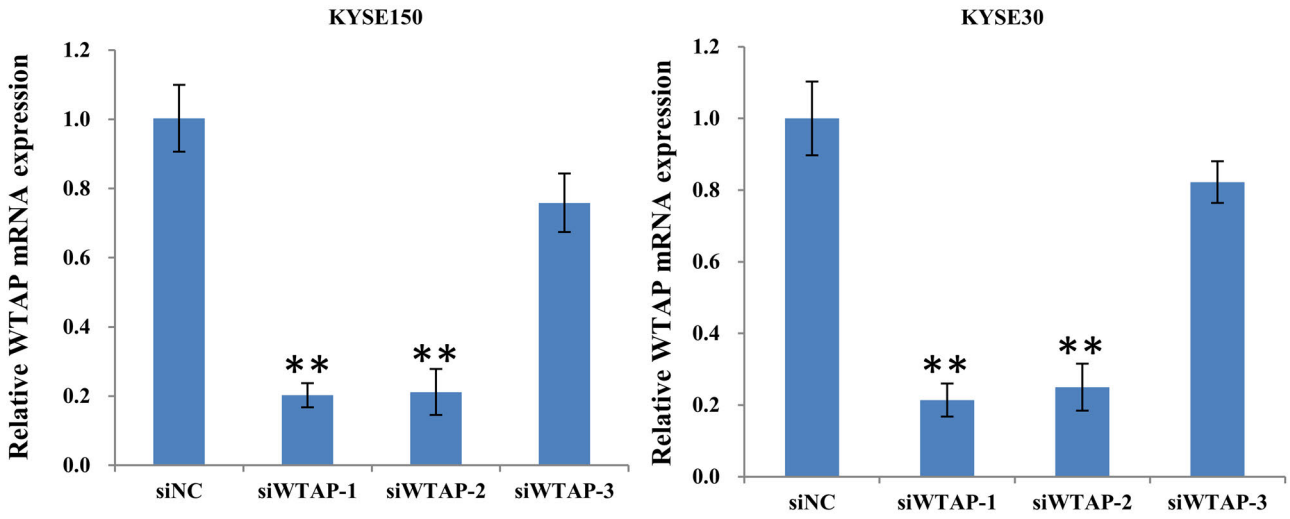

Supplementary Figure S1. A) Expression of WTAP in KYSE150 after transfection of siWTAP-1, siWTAP-2 and siWTAP-3; B) Expression of WTAP in KYSE30 after transfection of siWTAP-1, siWTAP-2 and siWTAP-3.